Electronic supplementary information

Diarylmaleic anhydrides: unusual organic luminescence, multi-stimuli response and photochromism

Xiaofei Mei[a], Jingwei Wang[b], Zhonggao Zhou[a], Shiyi Wu[b], Limei Huang[a], Zhenghuan Lin[b,*] and Qidan Ling[a,b,*]

[a] *College of Chemistry and Chemical Engineering, Fujian Normal University, Fuzhou 350007, Fujian, China.*

[b] *Fujian Key Laboratory of Polymer Materials, College of Materials Science and Engineering, Fujian Normal University, Fuzhou 350007, Fujian, China.*

**E-mail: zhlin@fjnu.edu.cn; qdling@fjnu.edu.cn*

Contents

1. Supplemental Schemes, figures and tables

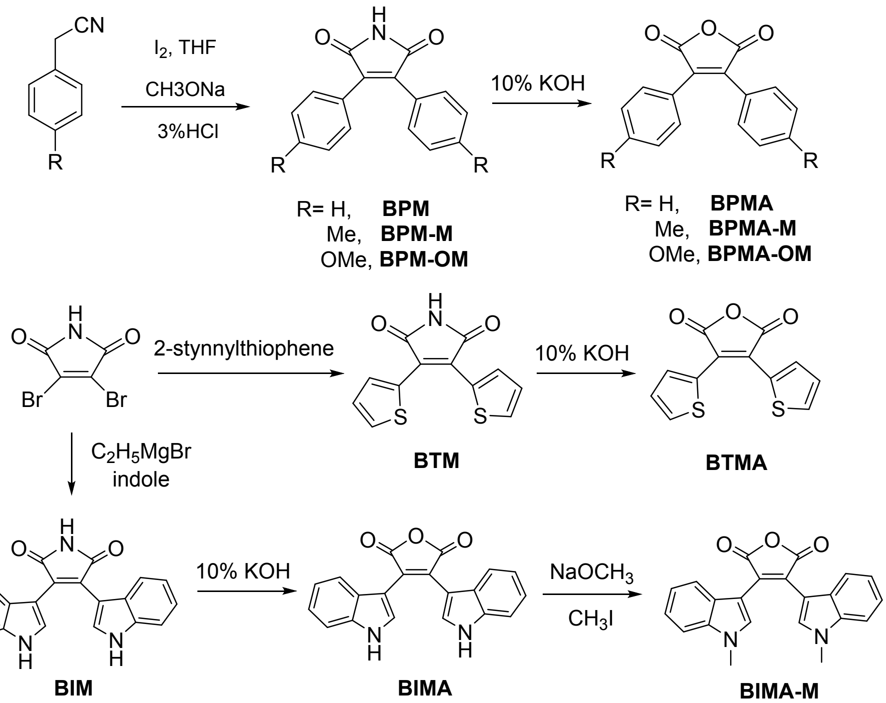

Scheme S1 Synthetic routes of diarylmaleic anhydrides.

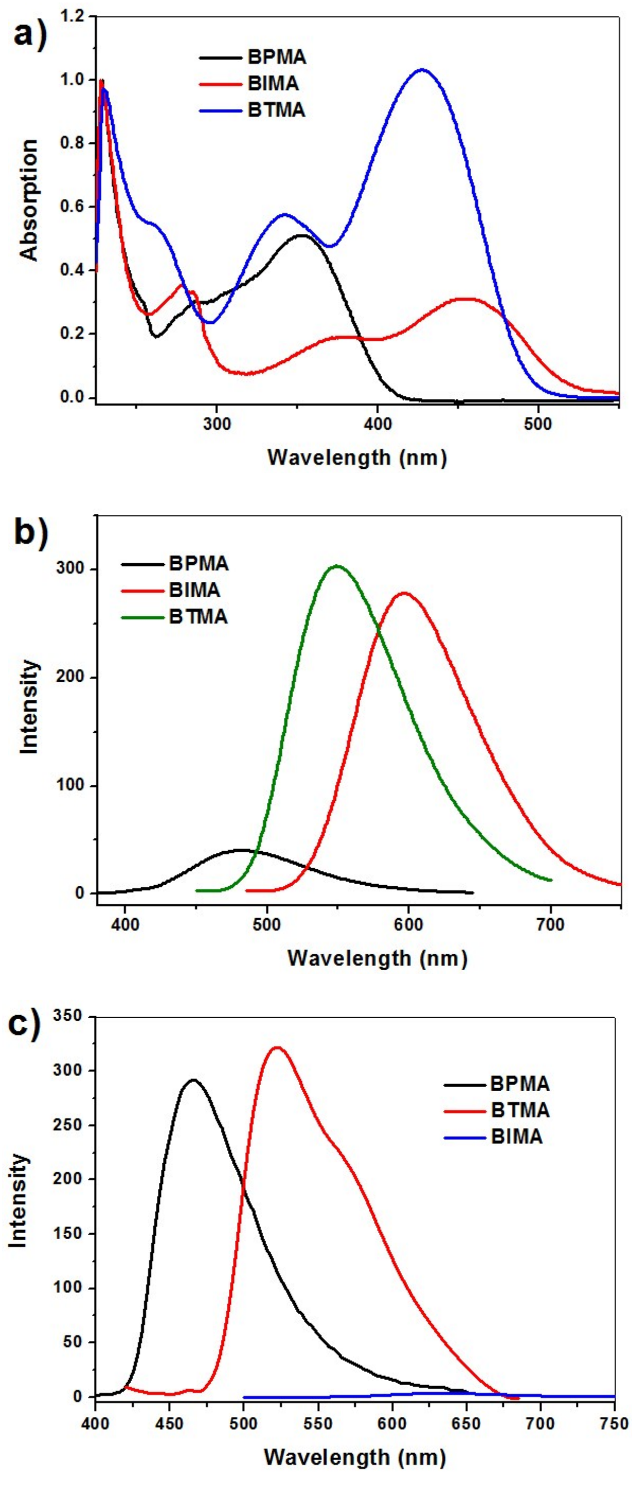

Fig. S1 Absorption (a) and emission (b) spectra of BPMA, BIMA, and BTMA in DCM solution. Emission spectra (c) of BPMA, BIMA, and BTMA in solid

Table S1 Calculated wavelength (λ) and oscillator strength (f) for absorption of BPMA, BTMA and BIMA.

Compounds		**Main orbital transition (CIC)** [a]	**λ, nm** [b]	***f*** [c]
BPMA	$S_0 \rightarrow S_1$	HOMO→LUMO (0.66)	393	0.2081
	$S_0 \rightarrow S_2$	HOMO-4→LUMO (-0.40) HOMO-1→LUMO (0.56)	359	0.0267
	$S_0 \rightarrow S_3$	HOMO-4→LUMO (0.57) HOMO-1→LUMO (0.41)	338	0.0143
BTMA	$S_0 \rightarrow S_1$	HOMO→LUMO (0.71)	460	0.3046
	$S_0 \rightarrow S_2$	HOMO-4→LUMO (0.28) HOMO-1→LUMO (0.65)	367	0.0148
	$S_0 \rightarrow S_3$	HOMO-3→LUMO (0.28) HOMO-2→LUMO (0.64)	349	0.0003
BIMA	$S_0 \rightarrow S_1$	HOMO→LUMO (0.70)	478	0.2043
	$S_0 \rightarrow S_2$	HOMO-2→LUMO (-0.16) HOMO-1→LUMO (0.68)	400	0.0798
	$S_0 \rightarrow S_3$	HOMO-2→LUMO (0.69)	379	0.0211

[a] CI expansion coefficients for the main orbital transitions. [b] Wavelength. [c] Oscillator strength.

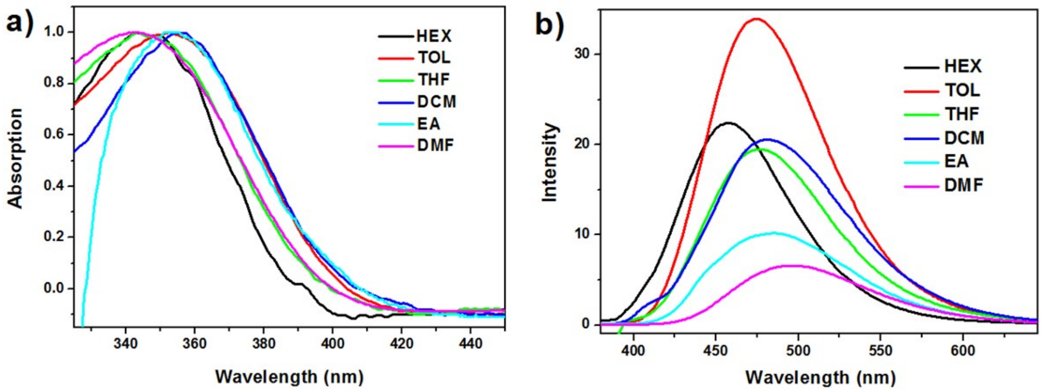

Fig. S2 Solvent effect on the absorption (a) and emission (b) spectra of BPMA: hexane (HEX), toluene (TOL), tetrahydrofuran (THF), dichloromethane (DCM), ethyl acetate (EA) and dimethyl formamide (DMF).

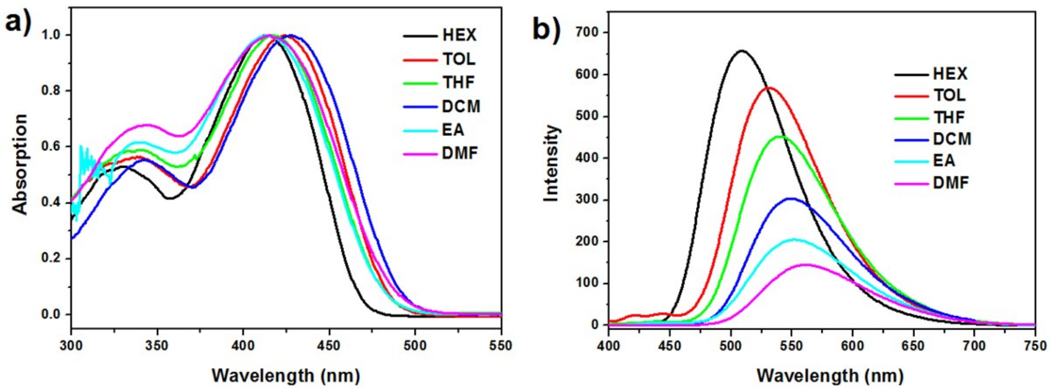

Fig. S3 Solvent effect on the absorption (a) and emission (b) spectra of BTMA: hexane (HEX), toluene (TOL), tetrahydrofuran (THF), dichloromethane (DCM), ethyl acetate (EA) and dimethyl formamide (DMF).

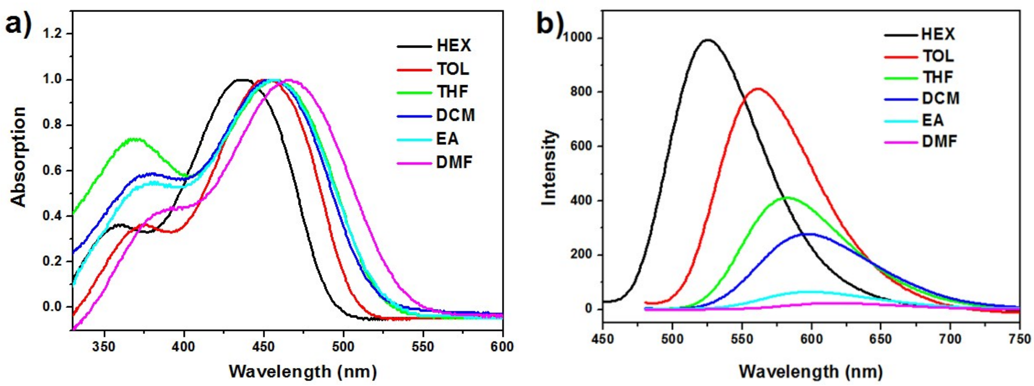

Fig. S4 Solvent effect on the absorption (a) and emission (b) spectra of BIMA: hexane (HEX), toluene (TOL), tetrahydrofuran (THF), dichloromethane (DCM), ethyl acetate (EA) and dimethyl formamide (DMF).

Table S2 Experimental data of photophysical properties of diarylmaleic anhydrides in different solutions

Compound	Solvent	λ_{abs} (nm)	λ_{em} (nm)	Stokes shift (nm)	Φ_F(%)
BPMA	HEX	344	457	113	2.5
	TOL	352	472	120	3
	THF	343	474	131	2.3
	DCM	356	479	123	2
	EA	355	484	129	1.5
	DMF	343	498	155	<0.1
BTMA	HEX	413	509	96	98
	TOL	423	531	108	82
	THF	418	540	122	71
	DCM	428	549	121	59
	EA	414	552	138	48
	DMF	415	561	146	40
BIMA	HEX	434	525	91	80
	TOL	448	561	113	75
	THF	452	582	130	58
	DCM	456	597	141	46
	EA	457	599	142	15
	DMF	436	617	181	8

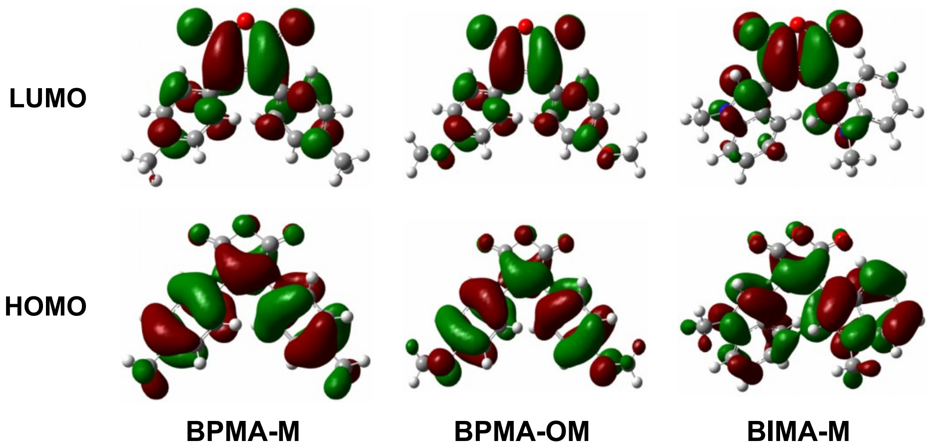

Figure S5. Orbital plots of BPMA-M, BPMA-OM and BIMA-M in the optimized structure.

Table S3 Calculated wavelength (λ) and oscillator strength (f) for absorption of BPMA-M, BPMA-OM and BIMA-M.

Compounds		**Main orbital transition (CIC)** [a]	**λ, nm** [b]	***f*** [c]
BPMA-M	$S_0 \rightarrow S_1$	HOMO→LUMO (0.70)	411	0.2617
	$S_0 \rightarrow S_2$	HOMO-4→LUMO (0.40) HOMO-1→LUMO (0.57)	359	0.0153
	$S_0 \rightarrow S_3$	HOMO-4→LUMO (0.57) HOMO-1→LUMO (-0.40)	337	0.0093
BPMA-OM	$S_0 \rightarrow S_1$	HOMO→LUMO (0.70)	450	0.3155
	$S_0 \rightarrow S_2$	HOMO-1→LUMO (0.70)	361	0.1086
	$S_0 \rightarrow S_3$	HOMO-4→LUMO (0.51) HOMO-2→LUMO (-0.47)	350	0.0023
BIMA-M	$S_0 \rightarrow S_1$	HOMO→LUMO (0.70)	490	0.2337
	$S_0 \rightarrow S_2$	HOMO-2→LUMO (-0.17) HOMO-1→LUMO (0.67)	400	0.0833
	$S_0 \rightarrow S_3$	HOMO-2→LUMO (0.68) HOMO-1→LUMO (0.17)	378	0.0235

[a] CI expansion coefficients for the main orbital transitions. [b] Wavelength. [c] Oscillator strength.

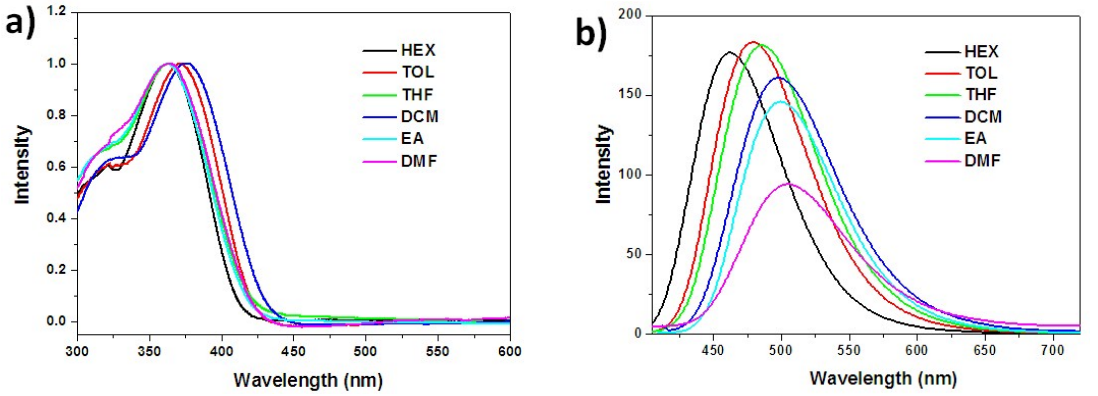

Fig. S6 Solvent effect on the absorption (a) and emission (b) spectra of BPMA-M: hexane (HEX), toluene (TOL), tetrahydrofuran (THF), dichloromethane (DCM), ethyl acetate (EA) and dimethyl formamide (DMF).

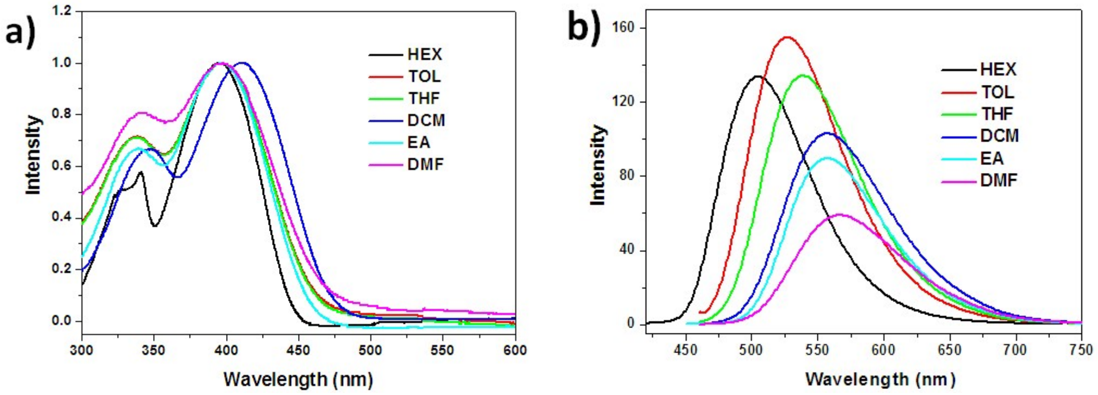

Fig. S7 Solvent effect on the absorption (a) and emission (b) spectra of BPMA-OM: hexane (HEX), toluene (TOL), tetrahydrofuran (THF), dichloromethane (DCM), ethyl acetate (EA) and dimethyl formamide (DMF).

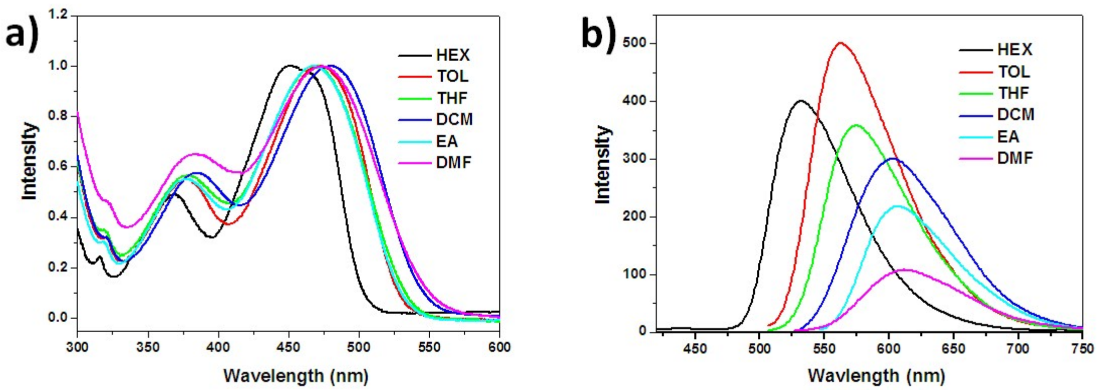

Fig. S8 Solvent effect on the absorption (a) and emission (b) spectra of BIMA-M: hexane (HEX), toluene (TOL), tetrahydrofuran (THF), dichloromethane (DCM), ethyl acetate (EA) and dimethyl formamide (DMF).

Table S4 Experimental data of photophysical properties of diarylmaleic anhydrides in different solutions

Compound	Solvent	λ_{abs} (nm)	λ_{em} (nm)	Stokes shift (nm)	Φ_F(%)
BPMA-M	HEX	363	457	94	53
	TOL	369	472	103	72
	THF	361	474	113	68
	DCM	374	498	105	48
	EA	362	484	122	42
	DMF	361	498	137	30
BPMA-OM	HEX	393	502	109	80
	TOL	394	526	132	98
	THF	391	538	147	71
	DCM	409	556	157	67
	EA	396	558	162	48
	DMF	395	567	172	38
BIMA-M	HEX	454	530	76	76
	TOL	470	562	92	82
	THF	468	573	105	52
	DCM	481	602	121	42
	EA	467	606	139	36
	DMF	465	614	149	27

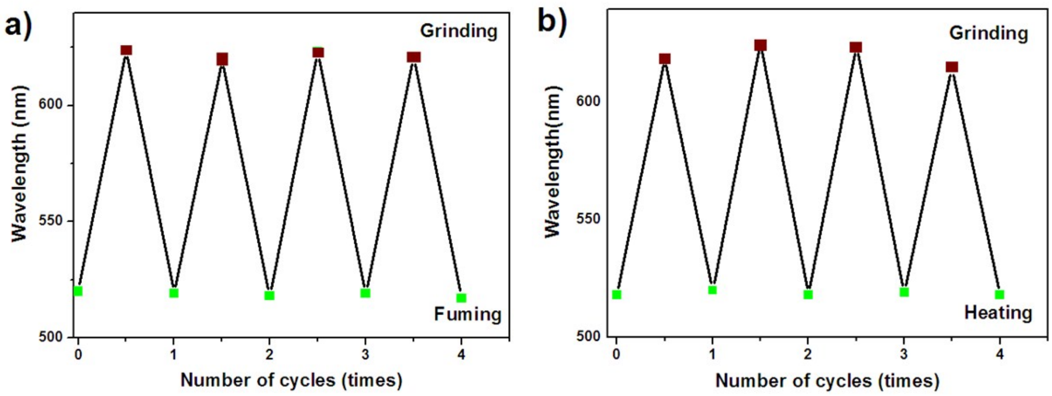

Fig. S9 Repeated switching between green and brown emission by fuming-grinding cycles (a) and heating-grinding cycles (b).

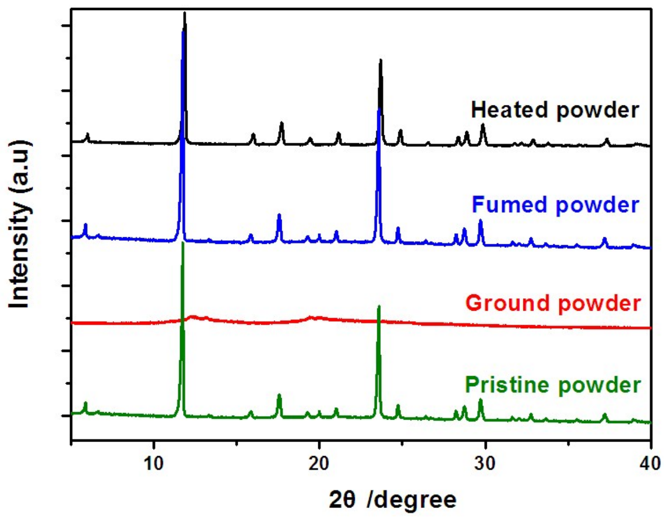

Fig. S10 The PXRD pattern of BTMA in pristine, ground, fumed and heated powder.

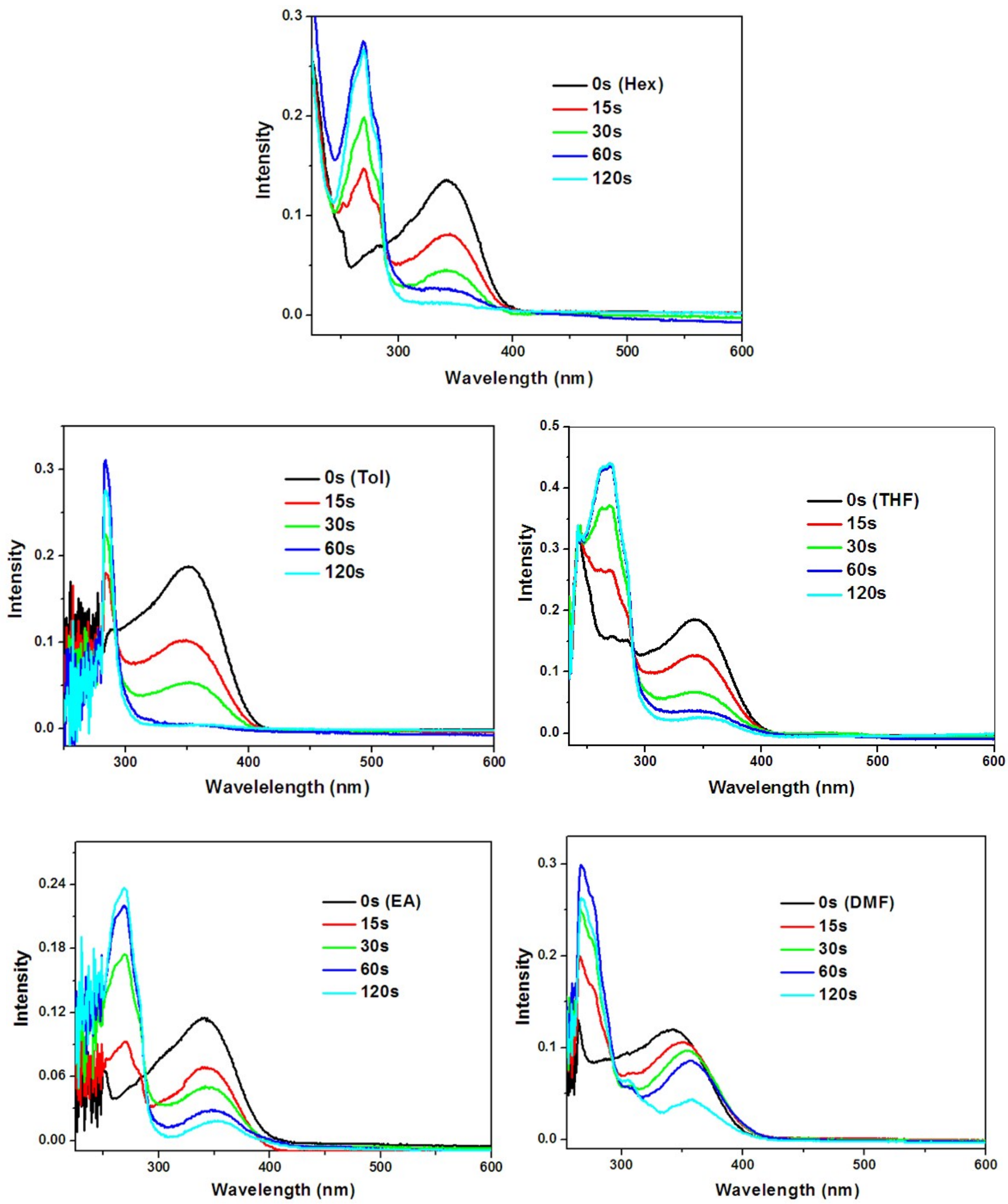

Fig. S11 Absorption spectra of BPMA in hexane (Hex), toluene (Tol), THF, ethyl acetate (EA) and DMF solvents under different irradiation time (365 nm).

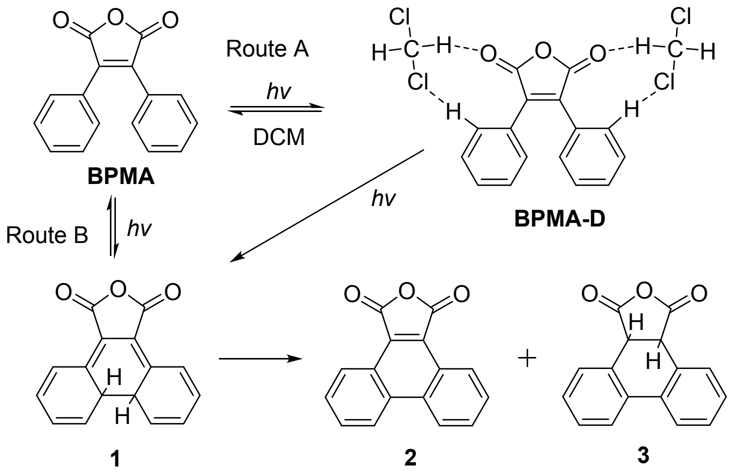

Scheme S2 Reaction route of the photo cyclization of BPMA.

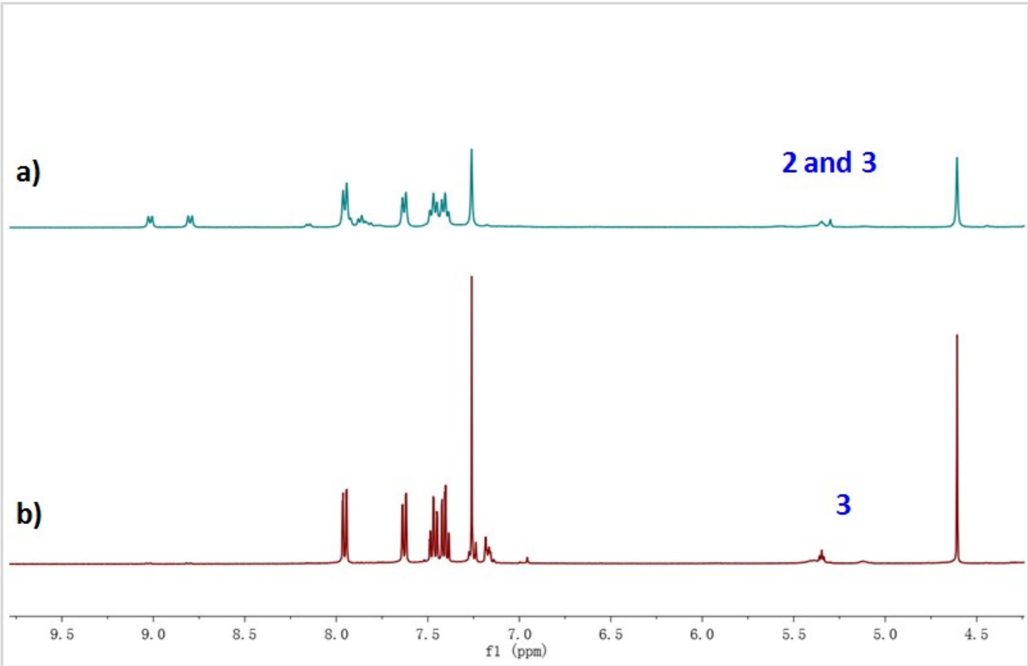

Fig. S12 ¹HNMR of the crude product of BPMA under the irradiation of 365 nm UV light for 4 h in the presence (a) and absence (b) of oxygen.

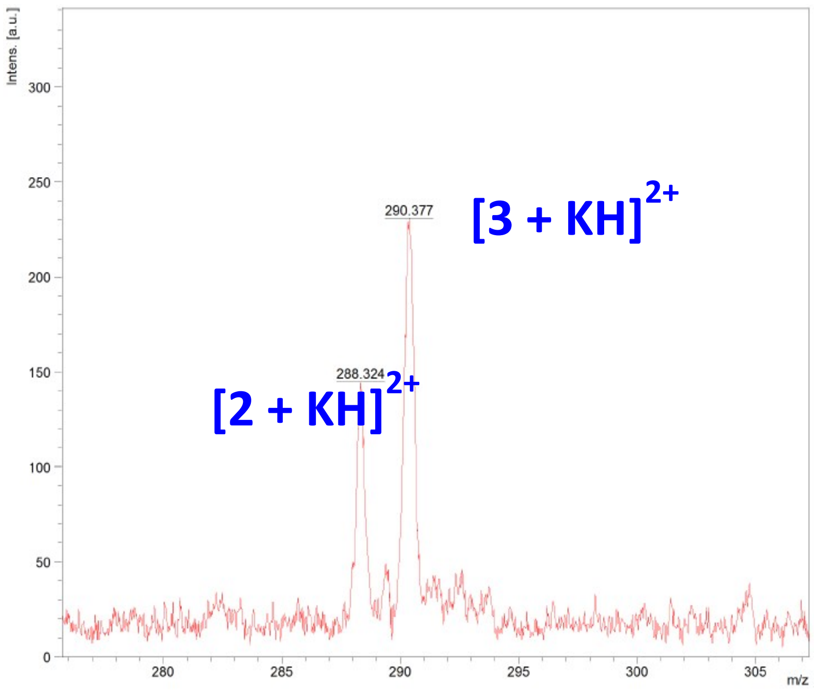

Fig. S13 MALDI-TOF mass spectra of the crude product of BPMA under the irradiation of 365 nm UV light for 4 h in the presence of oxygen.

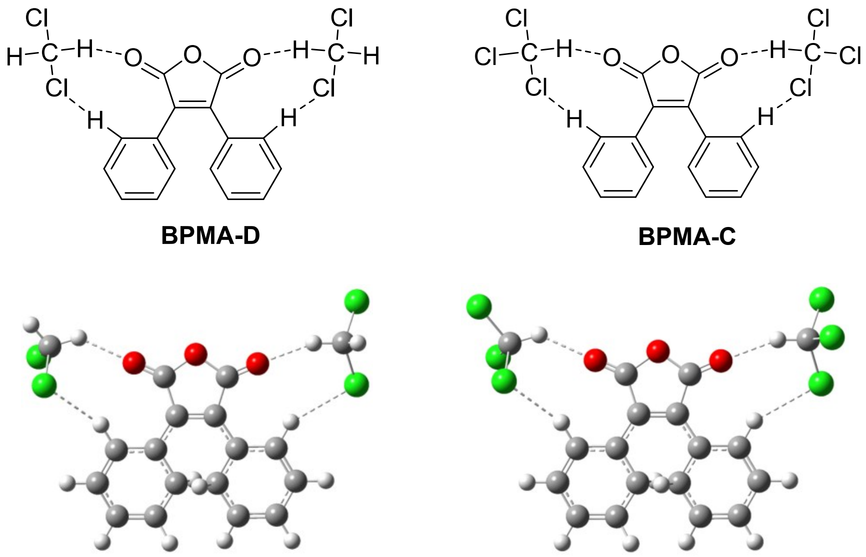

Fig. S14 Structure of the intermediates BPMA-D and BPMA-C, and their planar conformation.

Table S5 Calculated absorption parameters for planar BPMA-D and BPMA-C.

		Main orbital transition[a] (CIC)	λ (nm)[b]	f[c]
Planar BPMA-D	$S_0 \rightarrow S_2$	HOMO→LUMO+1 (0.34) HOMO→LUMO+2 (0.54)	504.8	0.0274
	$S_0 \rightarrow S_3$	HOMO→LUMO+1 (0.58) HOMO→LUMO+2 (-0.37)	501.4	0.0659
	$S_0 \rightarrow S_5$	HOMO-1→LUMO (0.39) HOMO→LUMO+6 (0.53)	399.8	0.0598
	$S_0 \rightarrow S_{10}$	HOMO-1→LUMO (-0.34) HOMO→LUMO+6 (0.43)	331.2	0.5109
Planar BPMA-C	$S_0 \rightarrow S_2$	HOMO→LUMO+1 (0.35) HOMO→LUMO+2 (0.54)	507.9	0.0272
	$S_0 \rightarrow S_3$	HOMO→LUMO+1 (0.58) HOMO→LUMO+2 (-0.38)	502.8	0.0659
	$S_0 \rightarrow S_7$	HOMO-1→LUMO (0.38) HOMO→LUMO+6 (0.53)	399.7	0.0656
	$S_0 \rightarrow S_{10}$	HOMO-1→LUMO (-0.33) HOMO→LUMO+6 (0.44)	332.0	0.5120

[a] CI expansion coefficients for the main orbital transitions. [b] Wavelength. [c] Oscillator strength.

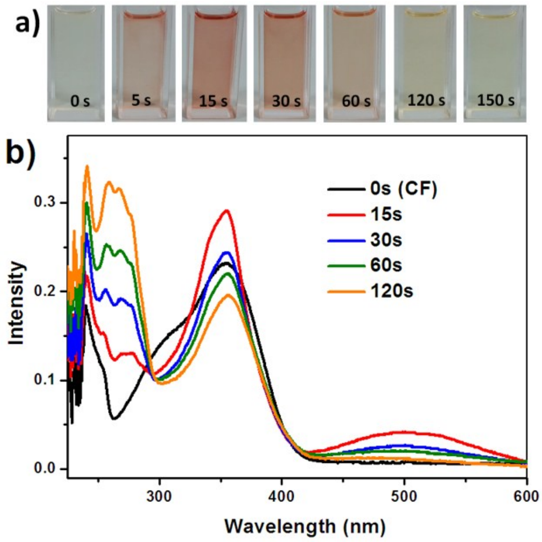

Fig. S15 Photochromic process of BPMA in CF under 365 nm UV light: a) photochromic phenomenon under irradiation for 0~150 s; b) Absorption spectra under different irradiation time.

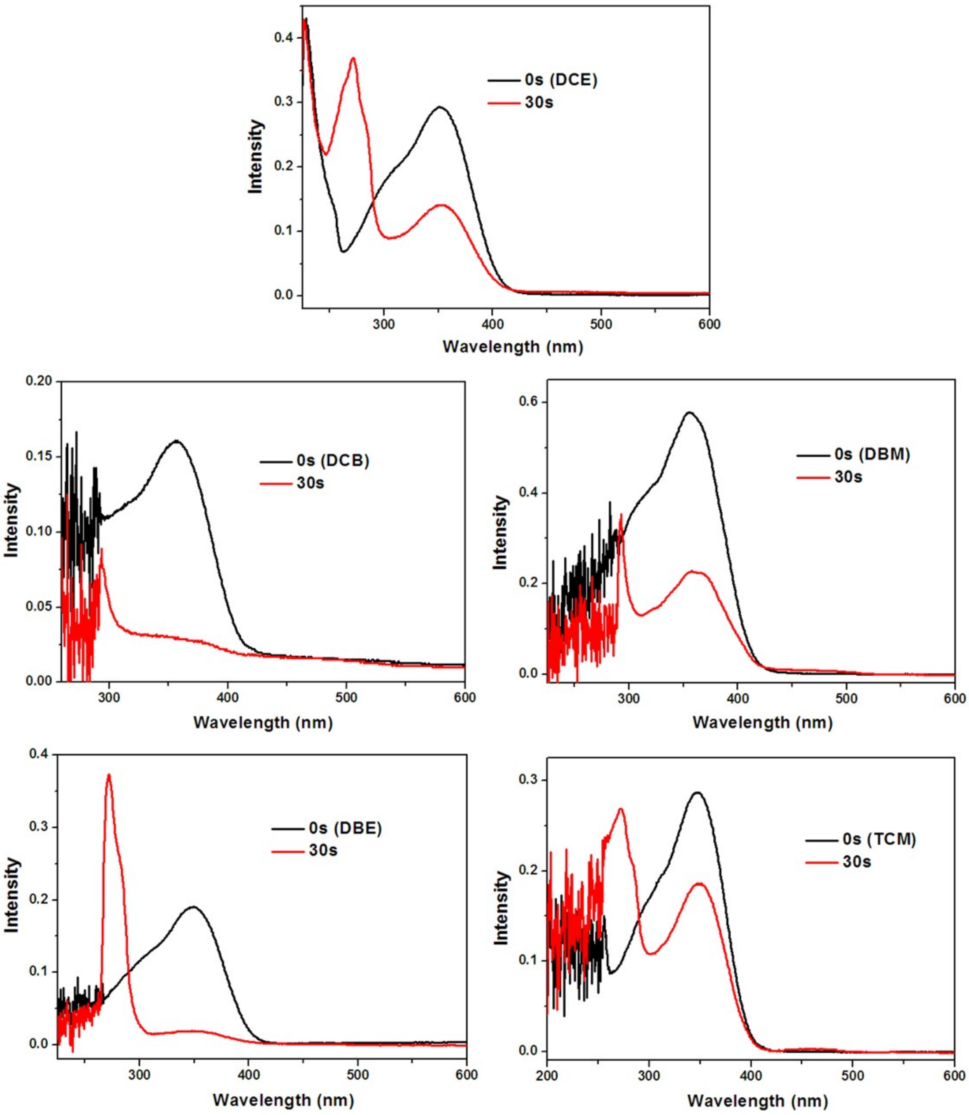

Fig. S16 Absorption spectra of BPMA in 1,2-dichloroethane (DCE), *o*-dichlorobenzene (DCB), dibromomethane (DBM), 1,2-dibromoethane (DBE) and tetrachloromethane (TCM) solvents under irradiation for 30s.

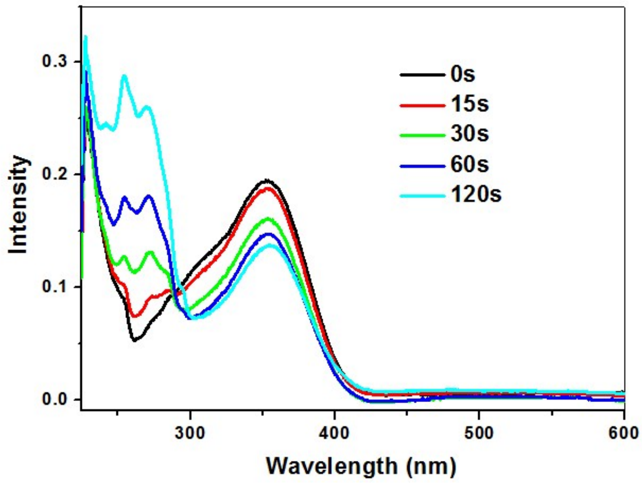

Fig. S17 Absorption spectra of BPMA in DCM solvent under irradiation of 254 nm UV light.

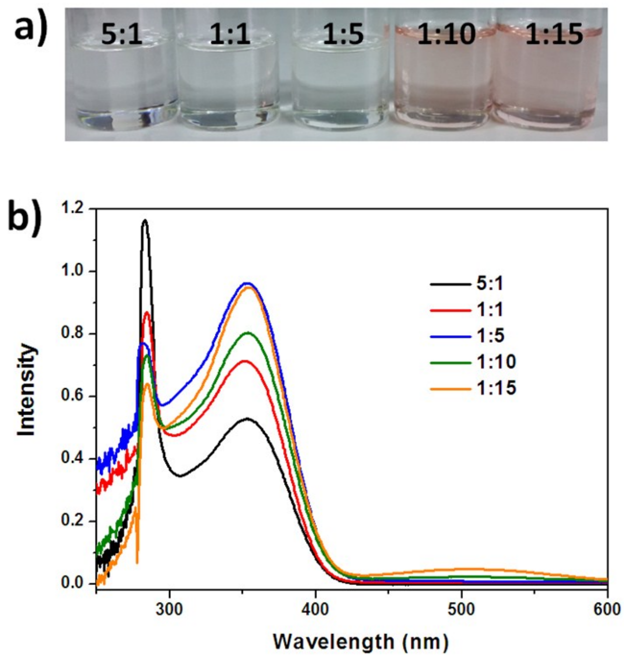

Fig. S18 Absorption spectra of BPMA in toluene/DCM (V_{tol}/V_{DCM}=5:1, 1:1, 1:5, 1:10 and 1:15) solvent under irradiation of 365 nm UV light.

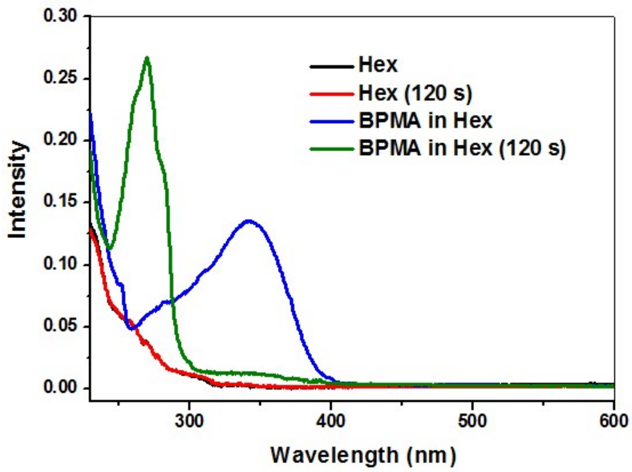

Fig. S19 Absorption of BPMA in hexane without and with 120 s of irradiation at 365 nm.

2. Experimental Section

General methods

High resolution ESI mass spectra were recorded on Bruker micrOTOF II spectrometer or a TSQ Quantum Access MAX of Thermo Fisher Scientific. MALDI-TOF mass spectra were recorded on a Bruker microflex LRF spectrometer. NMR spectra were measured in $CDCl_3$ or d-DMSO on a Bruker Ascend 400 FT-NMR spectrometer; ^1H and ^{13}C chemical shifts were quoted relative to the internal standard tetramethylsilane. UV-vis spectra were obtained on a Shimadzu UV-2600 spectrophotometer in the room temperature. The emission spectra were probed on a Shimadzu RF-5301PC fluorescence spectrophotometer. The thermal annealing processes were carried out in an oven. All photographs were recorded on a Canon Powershot G7 digital camera under UV light (365 nm). Powder X-ray diffraction (PXRD) data were collected using a PANalytical X-ray Diffractometer (X'Pert3 Powder) with Cu *Kα* radiation. The fluorescence lifetime and absolute quantum yield (Φ_F) values of solution and solid were measured using an Edinburgh Instruments FLS920 Fluorescence Spectrometer with a 6-inch integrating sphere except the Φ_F of BPMA in different solution determined against anthracene as a reference.[1]

X-ray crystallography

The single crystals of **BPMA**，**BIMA** and **BTMA** were mounted on a glass fiber for the X-ray diffraction analysis. Data sets were collected on an Agilent Technologies SuperNova Single Crystal Diffractometer equipped with graphite monochromatic Cu-*Kα* radiation (λ = 1.54184 Å). The single crystals were kept at 290.3 K during data collection. The structures were solved by SHELXS (direct methods) and refined by SHELXL (full matrix least-squares techniques) in the Olex2 package. All non-hydrogen atoms were refined anisotropically displacement parameters, and all hydrogen atoms in the ideal positions attached to their parent atoms. Crystallographic data for the structure of BPMA, BTMA and BIMA have been deposited in the Cambridge Crystallographic Data Centre as supplementary publication no. CCDC 1518041, 1518042 and 1518043, respectively.

Molecular simulations

Molecular Simulations were performed on Gaussian 09 program.[2] Geometry at ground state was fully optimized by the density functional theory (DFT) method with the Becke three-parameter hybrid exchange and the Lee-Yang-Parr correlation function (B3LYP) and 6-31G* basis set. The optical transitions were calculated by time-dependent density function (TD-DFT) theory with same function and basis set.

Materials and syntheses

All of the used reagents and solvents were obtained from commercial suppliers and used without further purification unless otherwise noted. 3,4-Dibromomaleimide was synthesized according to a previously reported method.[3] Thin layer chromatography was performed on G254 plates of Qingdao

Haiyang Chemical. Column chromatography was performed on Sorbent Technologies brand silica gel (40–63 mm, Standard grade).

Synthesis of BPMA, BPMA-M and BPMA-OM

An anhydrous THF (20 mL) solution of cyanide (6.8 mmol) and iodine (1.73 g, 6.8 mmol) was placed into -78 ^{o}C bath purged with N_2. Then, to the solution were slowly added 20 mL CH_3ONa solution (Na, 1 g, 43.7 mmol and methanol, 20 mL). The mixture was allowed to heat to ambient temperature and stirred for 10 h, then the mixture was neutralized by adding HCl solution (1 M) slowly. It was extracted for several times with dichloromethane and saturated NaCl aqueous solution, and then dried over anhydrous $MgSO_4$. After the solvent was removed under reduced pressure, the crude product was purified by silica gel column chromatography with DCM as eluent to give the green BPM and BPM-M, and yellow BPM-OM in 65~85% of isolated yield.

To an aqueous solution (100 mL) of 10% KOH was added BPM, BPM-M and BPM-OM (1 mmol). The mixture was heated to reflux for 4 h and then neutralized by the addition of hydrochloric acid (10 N) until precipitates formed. It was filtered, and the filtrates were dried in vacuo. The product was purified by recrystallization from ethanol, affording pure solids in 80~90% yield.

3,4-diphenylmaleic anhydride (BPMA). Yield: 80%. ^{1}H NMR (400 MHz, $CDCl_3$) δ 7.55 (d, J = 6.8 Hz, 4H), 7.47 (t, J = 7.6, 7.2 Hz, 2H), 7.41 (t, J = 7.6, 7.2 Hz, 4H). ^{13}C NMR (100 MHz, $CDCl_3$) δ 164.83, 138.18, 131.17, 129.71, 128.95, 127.19. MS (ESI) m/z $[M+H]^+$ calcd 251.0708, found 251.0705.

3,4-di(4-methylphenyl)maleic anhydride (BPMA-M). Yield: 87%. ^{1}H NMR (400 MHz, $CDCl_3$) δ 7.46 (d, J = 8.2 Hz, 4H), 7.20 (d, J = 8.0 Hz, 4H), 2.39 (s, 6H). ^{13}C NMR (100 MHz, $CDCl_3$) δ 165.13, 141.66, 137.35, 129.63, 129.61, 124.57, 21.60. MS (ESI) m/z $[M+Na]^+$ calcd 301.0841, found 301.0824.

3,4-di(4-methoxyphenyl)maleic anhydride (BPMA-OM) . Yield: 90%. ^{1}H NMR (400 MHz, $CDCl_3$) δ 7.56 (d, J = 8.8 Hz, 4H), 6.91 (d, J = 8.8 Hz, 4H), 3.85 (s, 6H). ^{13}C NMR (100 MHz, $CDCl_3$) δ 165.44, 161.69, 135.66, 131.44, 119.93, 114.43, 55.41. MS (ESI) m/z $[M+H]^+$ calcd 310.0841, found 310.0834.

Synthesis of 3,4-di(thiophen-2-yl)maleic anhydride (BTMA)

In 100 mL flask, 3,4-dibromomaleimide (1 g, 4 mmol), 2-tributylstannylthiophene (2.6 ml, 8.2 mmol), bis(triphenylphosphine)palladium(II) dichloride (0.14 g, 0.2 mmol) and anhydrous DMF (30 ml) were added. Then, the reaction mixture was heated to 90 °C for 10 h. The reaction mixture was cooled to room temperature and most of the solvent was evaporated. After purification by silica gel column chromatography employing DCM/hexane (1:1) as eluent, the yellow compound BTM (0.92g) was acquired in 90% total yield. ^{1}H NMR (400 MHz, *d*-DMSO): δ7.21 (t, J= 4 Hz, 2H), 7.72 (d, J = 4 Hz, 2H), 7.88 (d, J = 6 Hz, 2H), 11.37 (s, 1H).

To an aqueous solution (100 mL) of 10% KOH was added BTM (0.26 g, 1 mmol). The mixture was heated to reflux for 4 h and then neutralized by the addition of hydrochloric acid (10 N) until precipitates formed. It was filtered, and the filtrates were dried in vacuo. The product was purified by silica gel column chromatography with DCM/PE (1:2) as eluent, affording green solids of BTMA (0.23 g) in 88 % yield. ^{1}H NMR (400 MHz, $CDCl_3$) δ 7.99 (d, J = 2.8 Hz, 2H), 7.69 (dd, J = 4 Hz, 2H), 7.21 (dd, J = 4, 4.8 Hz, 2H). ^{13}C NMR (100 MHz, $CDCl_3$) δ 164.31, 132.84, 132.39, 128.82, 128.46, 128.07. MS (ESI) m/z $[M+H]^+$ calcd 262.9837, found 262.9832.

Synthesis of 3,4-di (indol-3-yl)maleimide (BIMA)

Mg (1.68 g, 0.07 mmol) was purged with N_2 before adding anhydrous THF (20 mL) in 500 mL flask. To a solution of Mg was added C_2H_5Br (5.2 ml, 0.07 mmol) slowly. The mixture was heated to 40℃. After 1 h， a solution of indole (7.8 g, 0.067 mol) in toluene was added to the flask. The mixture was heated to 60 °C. After 1 h, a solution of 3,4-dibromaleimide (3 g, 0.01 mol) in 150 mL toluene was added to the flask slowly. Then, the reaction mixture was heated to 120°C for 8 h. It was allowed to cool to ambient temperature and was filtered. The product was purified by silica gel column chromatography with EA/PE (1:4) as the eluant, affording dark red solids **BIM** (4.9 g) in 78 % yield.

To an aqueous solution (100 mL) of 10% KOH was added BIM (0.33 g, 1 mmol). The mixture was heated to reflux for 4 h and then neutralized by the addition of hydrochloric acid (10 N) until precipitates formed. It was filtered, and the filtrates were dried in vacuo. The product was purified by recrystallization from acetone, affording red-bulk solids (0.27 g) in 82 % yield. ^{1}H NMR (400 MHz, *d*-DMSO) δ 11.91 (s, 2H), 7.84 (s, 2H), 7.40 (d, J = 8.1 Hz, 2H), 7.02 (t, J = 7.2, 4.0 Hz, 2H), 6.83 (d, J = 8.0 Hz, 2H), 6.69 (t, J = 7.6 Hz, 7.2Hz 2H). ^{13}C NMR (100 MHz, $CDCl_3$) δ 166.67, 135.85, 129.49, 128.57, 125.07, 123.24, 122.07, 121.01, 111.47, 106.64. MS (ESI) m/z $[M+H]^+$ calcd 329.0926, found 329.0916.

Synthesis of 3,4-di(N-methyl-indol-3-yl)maleic anhydride(BIMA-M)

In 50 mL round bottom flask, a mixture of BIMA (0.33 g, 1 mmol), potassium tert-butoxide (0.47 g, 4.2 mmol), and anhydrous DMF (15 mL) was added and stirred for 1 h at 0 ℃, then methyl iodide (0.57 g, 4 mmol) was added quickly into the mixture. After stirring for 10 h, the mixture was poured into water. It was extracted for several times with dichloromethane, and then dried over anhydrous $MgSO_4$. After the solvent was removed under reduced pressure, the crude product was purified by silica gel column chromatography with DCM/PE (1:3) as eluent to give the yellow product in 78 % yield . ^{1}H NMR (400 MHz, $CDCl_3$) δ 7.77 (s, 2H), 7.32 (d, *J* = 8.1 Hz, 2H), 7.14 (t, *J* = 8, 8Hz, 2H), 6.91 (d, *J* = 7.9 Hz, 2H), 6.77 (t, J = 8.1, 8 Hz, 2H), 3.87 (s, 6H). ^{13}C NMR (100 MHz, $CDCl_3$) δ 167.02, 136.92, 133.78, 127.31, 125.97, 122.71, 122.40, 120.57, 109.65, 105.23, 33.50. MS (ESI) m/z $[M]^+$ calcd 356.1161, found 356.1166.

3. Structural Characterizations

Table S6 Crystal data and structure refinement for **BPMA**, **BTMA** and **BIMA**.

Crystal	**BPMA**	**BTMA**	**BIMA**
Formula	$C_{16}H_{10}O_3$	$C_{12}H_6O_3S_2$	$C_{20}H_{12}N_2O_3$
Formula weight	250.24	262.31	328.32
Crystal system	Monoclinic	Monoclinic	Monoclinic
Space group	P 1 21/c 1	P 1 21/c 1	P 1 c 1
a (Å)	15.2208(4)	15.1632(4)	7.2537(3)
b (Å)	5.94826(19)	5.75337(13)	6.7653(3)
c (Å)	13.8485(4)	12.5157(3)	15.6473(7)
α(deg)	90.00	90.00	90.00
β(deg)	101.601(3)	95.460(2)	97.694(4)
γ(deg)	90.00	90.00	90.00
V (Å^3)	1228.19(6)	1086.91(4)	760.95(6)
Z	4	4	2
$D_{calcd.}$(g/cm^3)	1.353	1.6029	1.433
F(000)	520.0	540.2109	340.0
R (int)	0.0154	0.0687	0.0415
GOF on F^2	1.102	1.0495	1.061
R1[I > 2σ(I)]	0.0505	0.0599	0.0580
wR2[I>2σ(I)]	0.1179	0.1599	0.1556
R1 (all data)	0.0595	0.0667	0.0608
wR2(all data)	0.1278	0.1721	0.1598

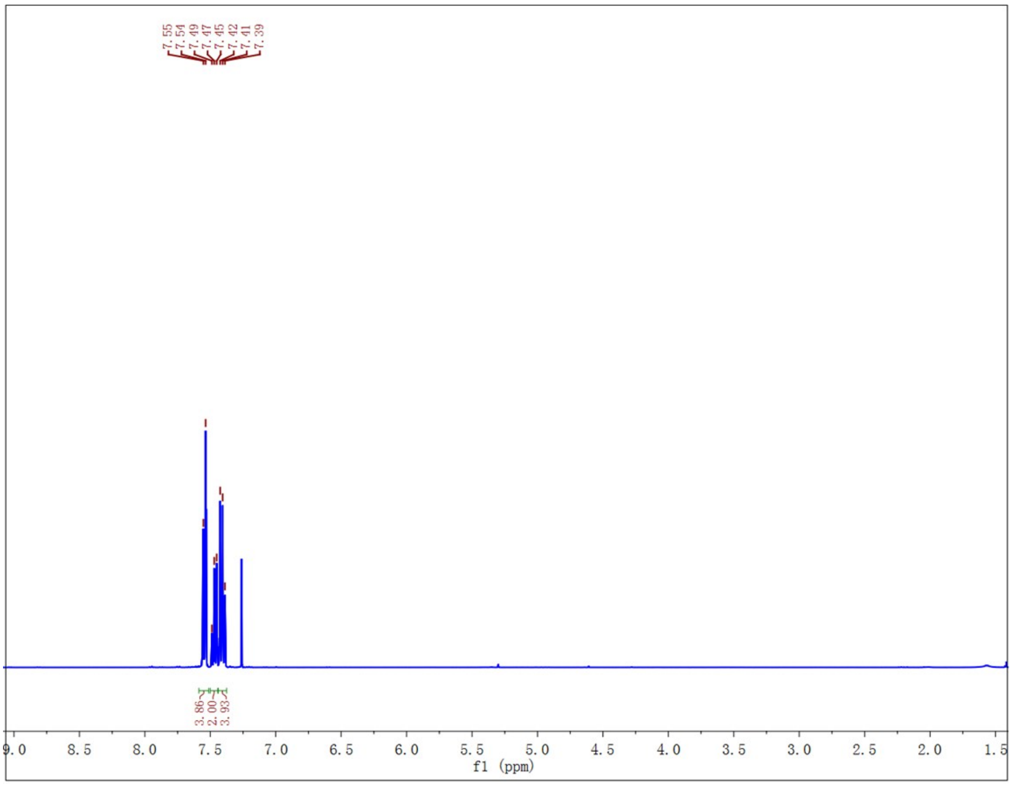

Fig. S20 ^{1}H NMR of BPMA in *d*-$CDCl_3$.

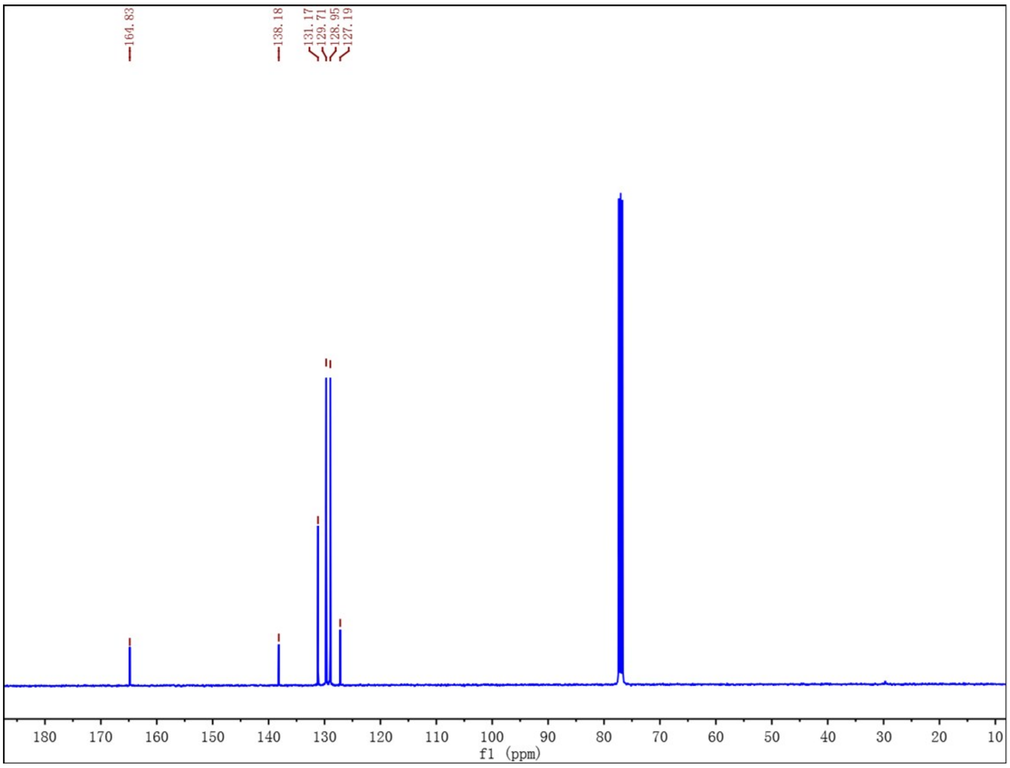

Fig. S21 ^{13}C NMR of BPMA in *d*-$CDCl_3$.

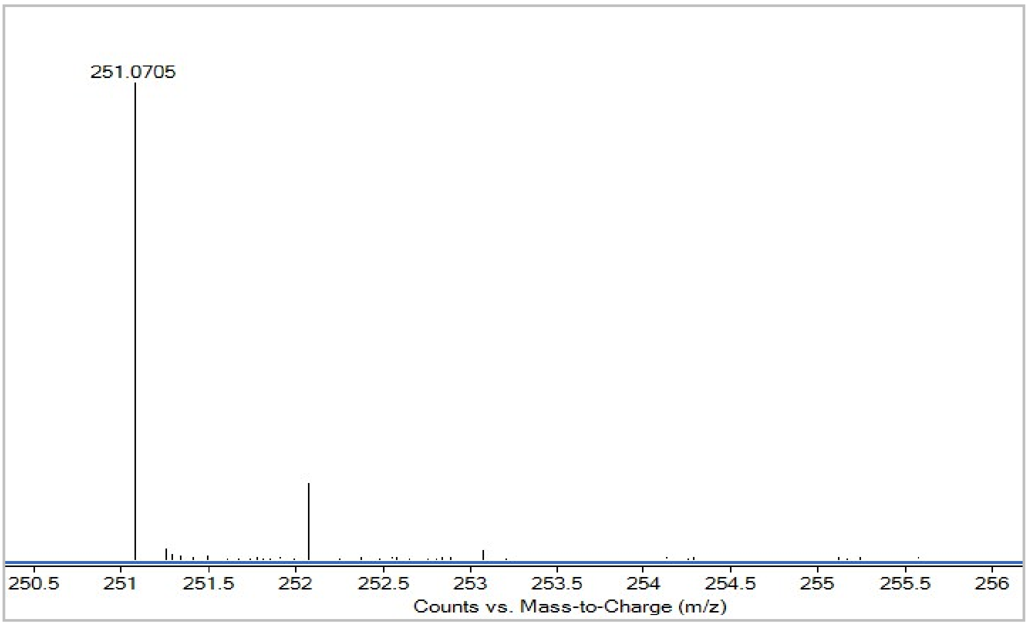

Fig. S22 High-resolution Mass of BPMA.

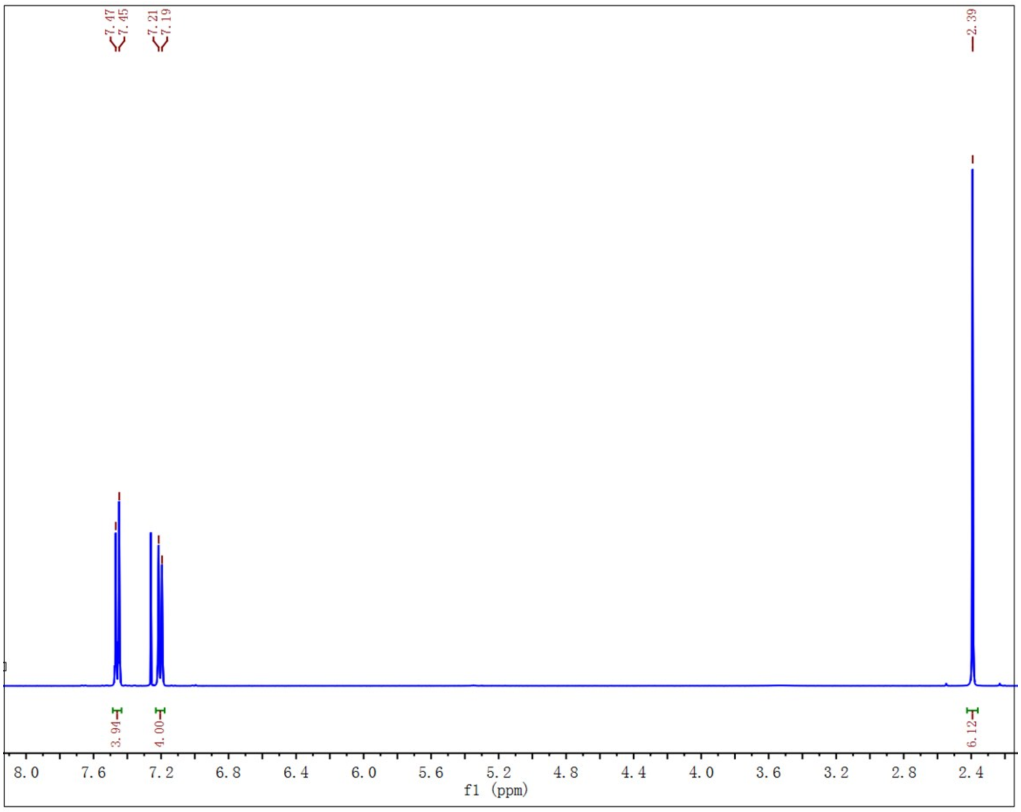

Fig. S23 ^{1}H NMR of BPMA-M in *d*-$CDCl_3$.

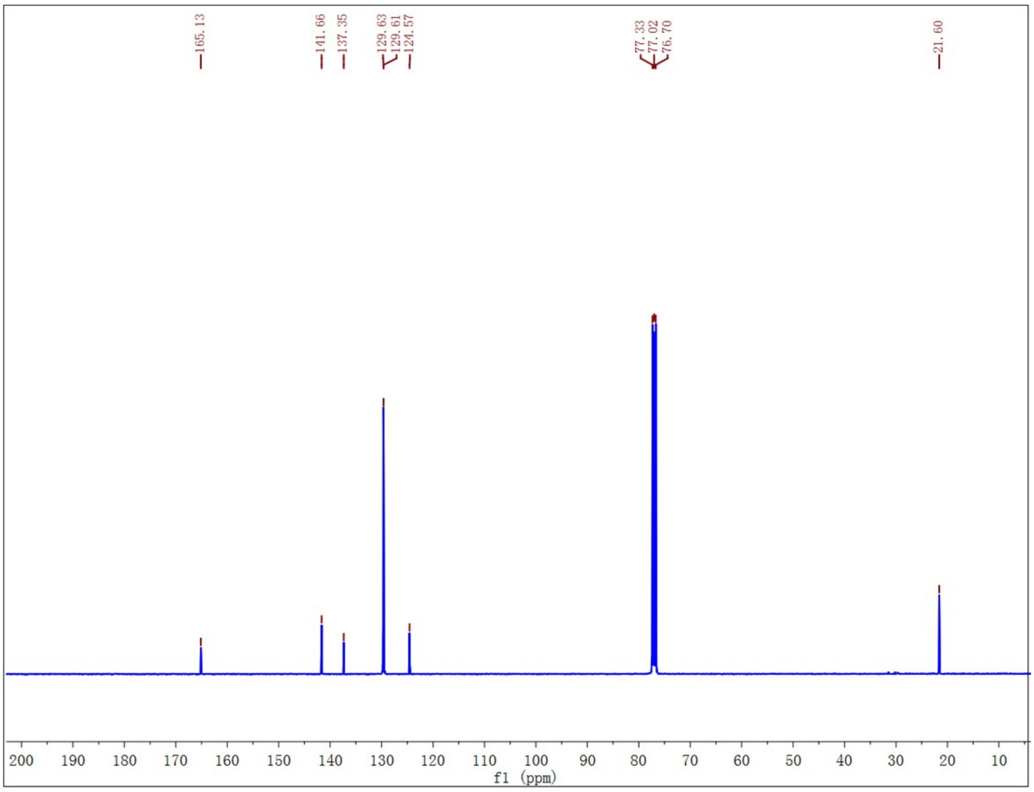

Fig. S24 ^{13}C NMR of BPMA-M in *d*-$CDCl_3$

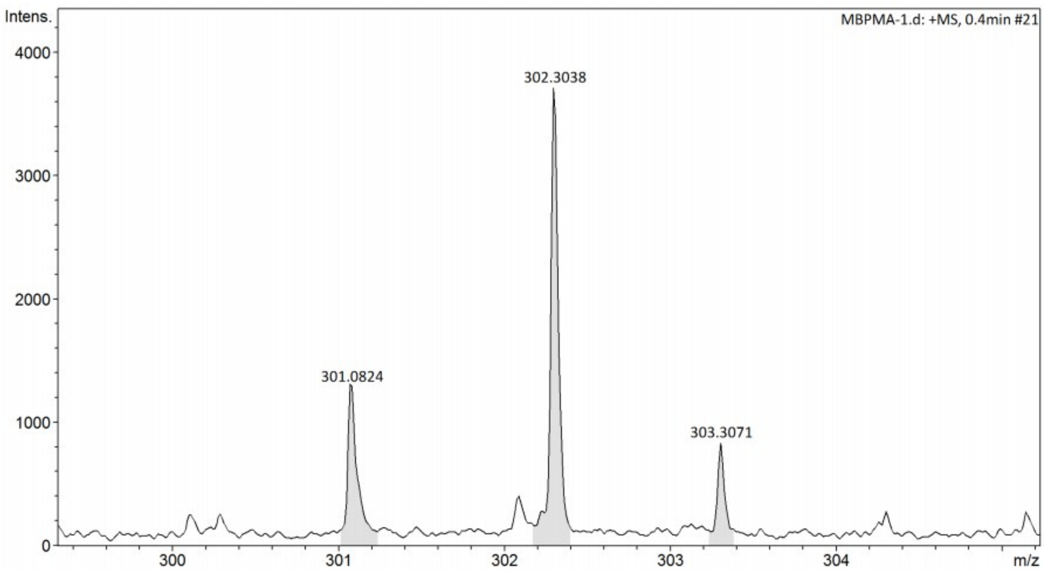

Fig. S25 High-resolution Mass of BPMA-M.

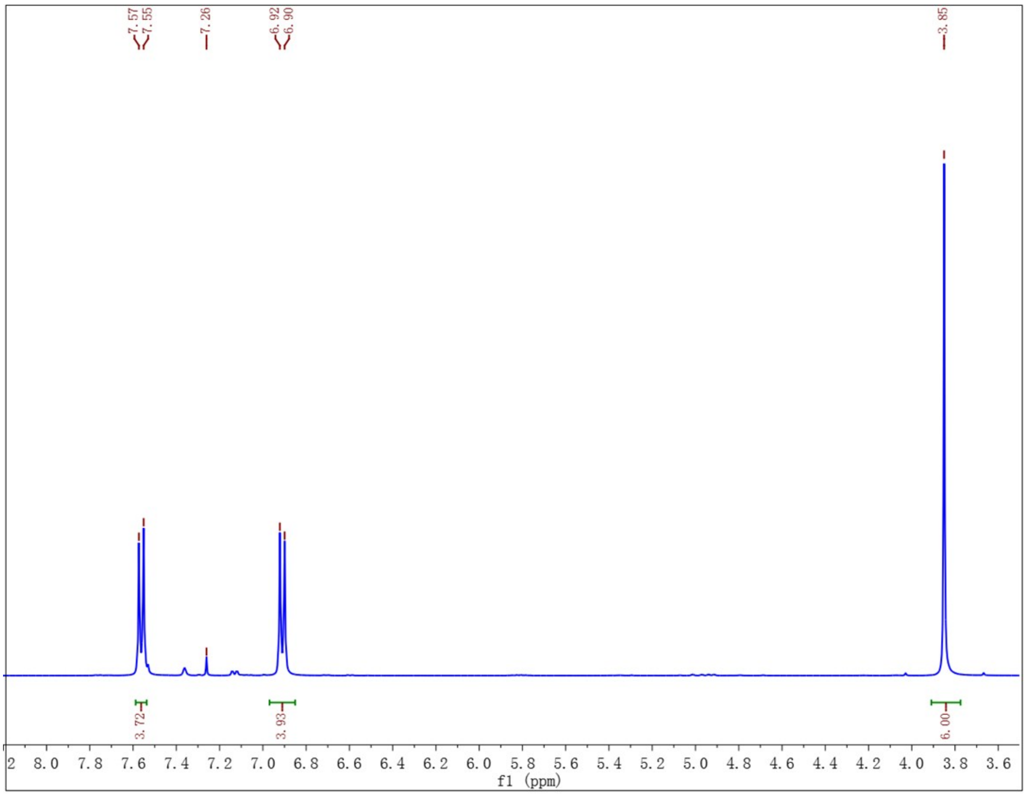

Fig. S26 ^{1}H NMR of BPMA-OM in *d*-$CDCl_3$.

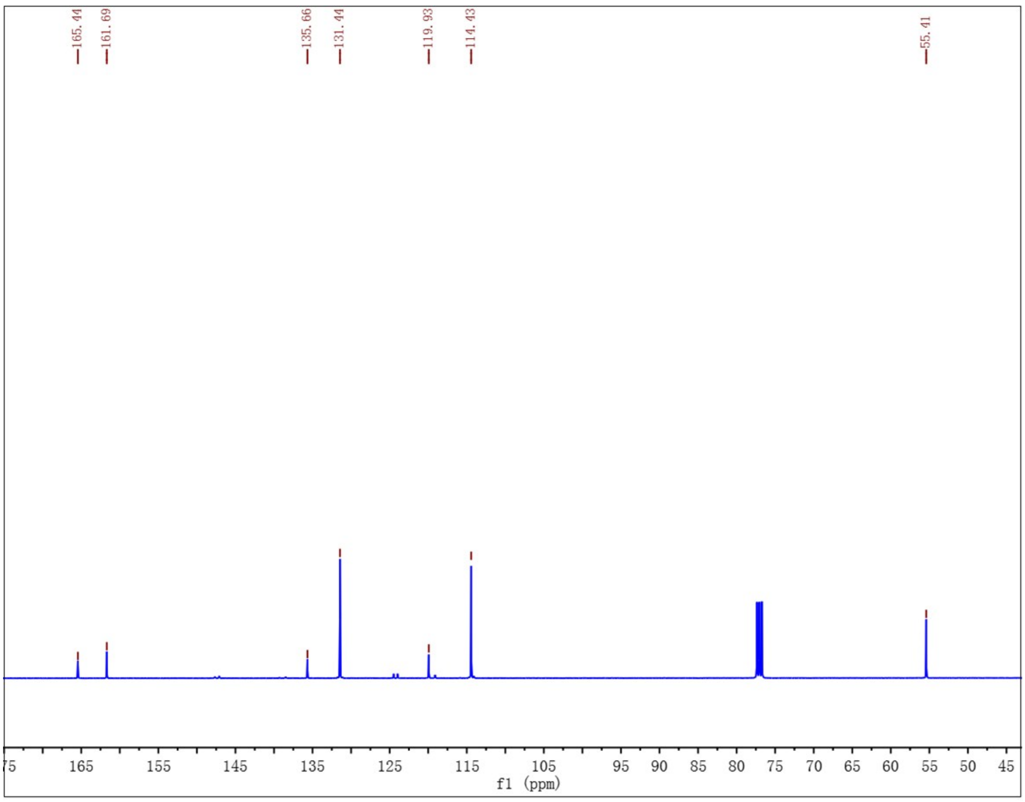

Fig. S27 ^{13}C NMR of BPMA-OM in *d*-$CDCl_3$.

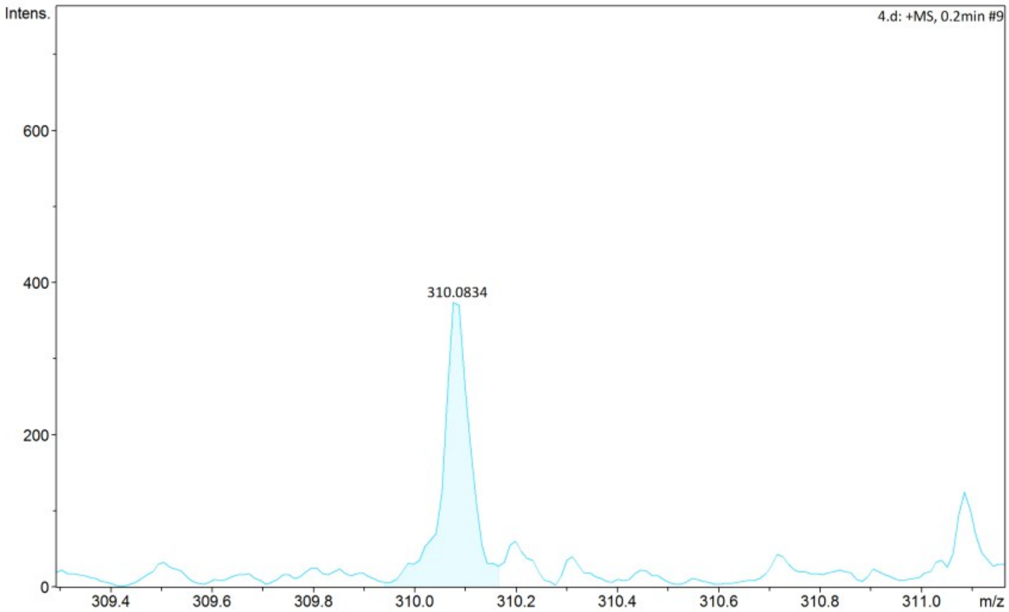

Fig. S28 High-resolution Mass of BPMA-OM.

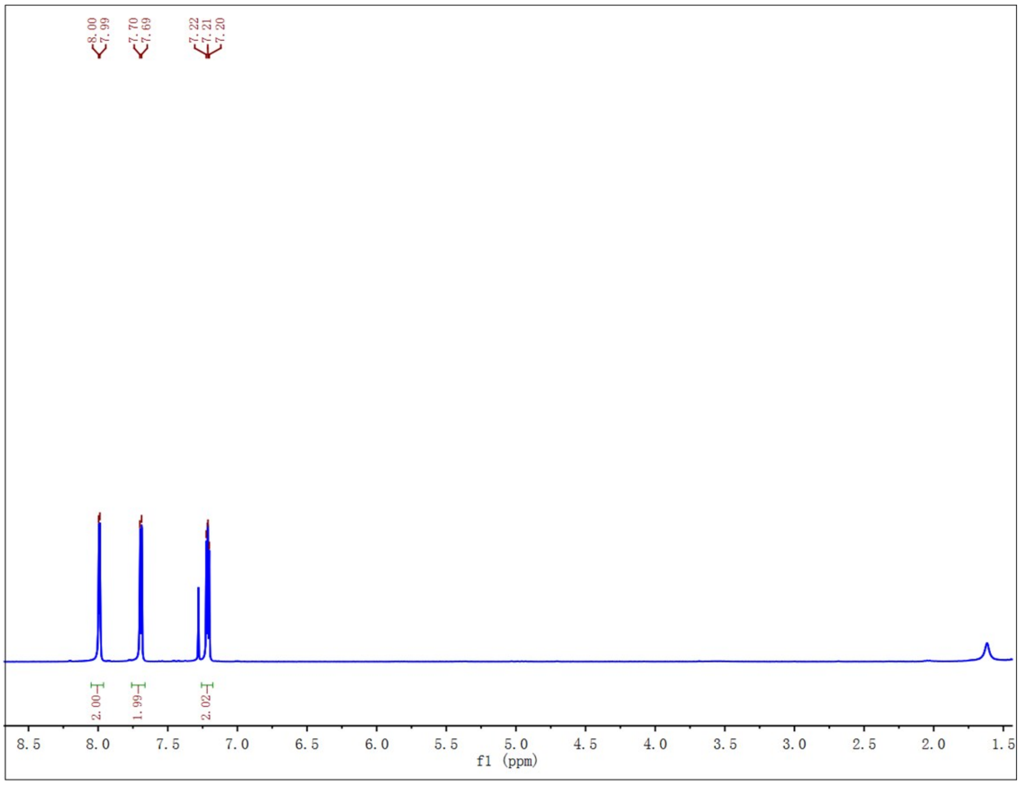

Fig. S29 ^{1}H NMR of BTMA in *d*-$CDCl_3$.

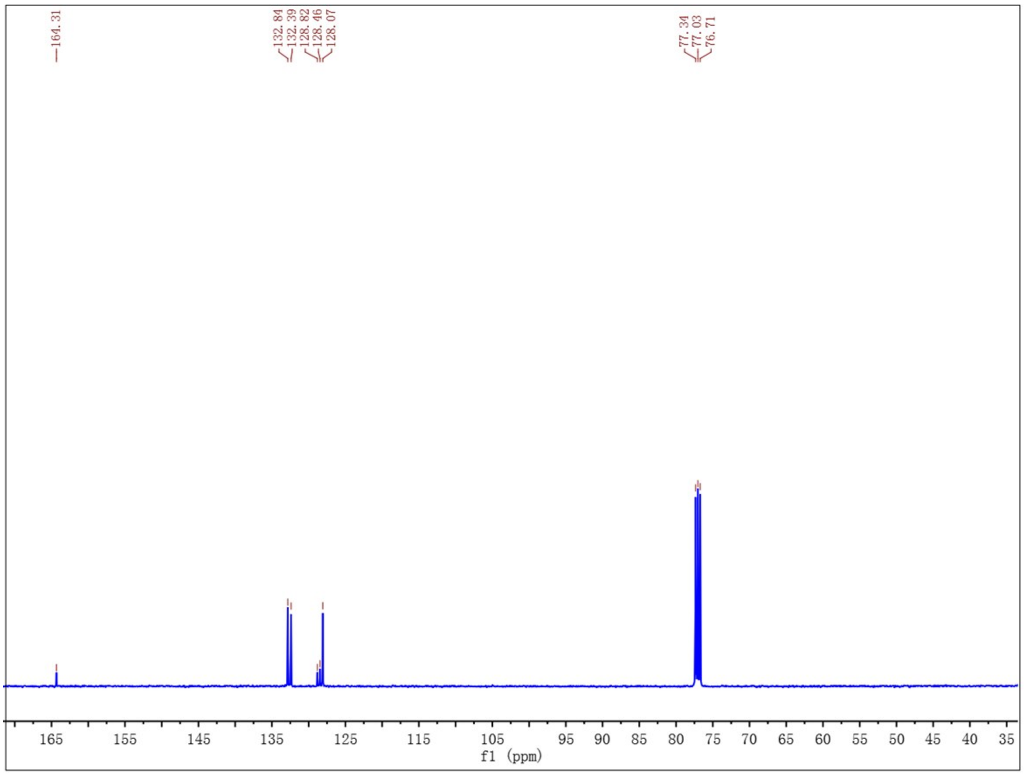

Fig. S30 ^{13}C NMR of BTMA in *d*-$CDCl_3$.

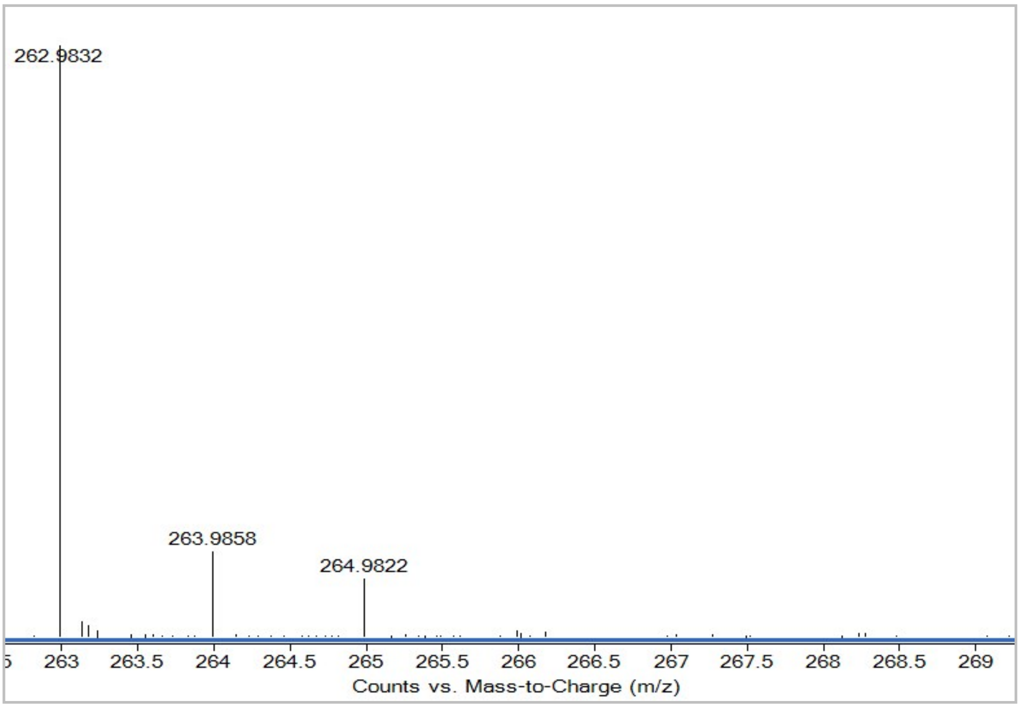

Fig. S31 High-resolution Mass of BTMA.

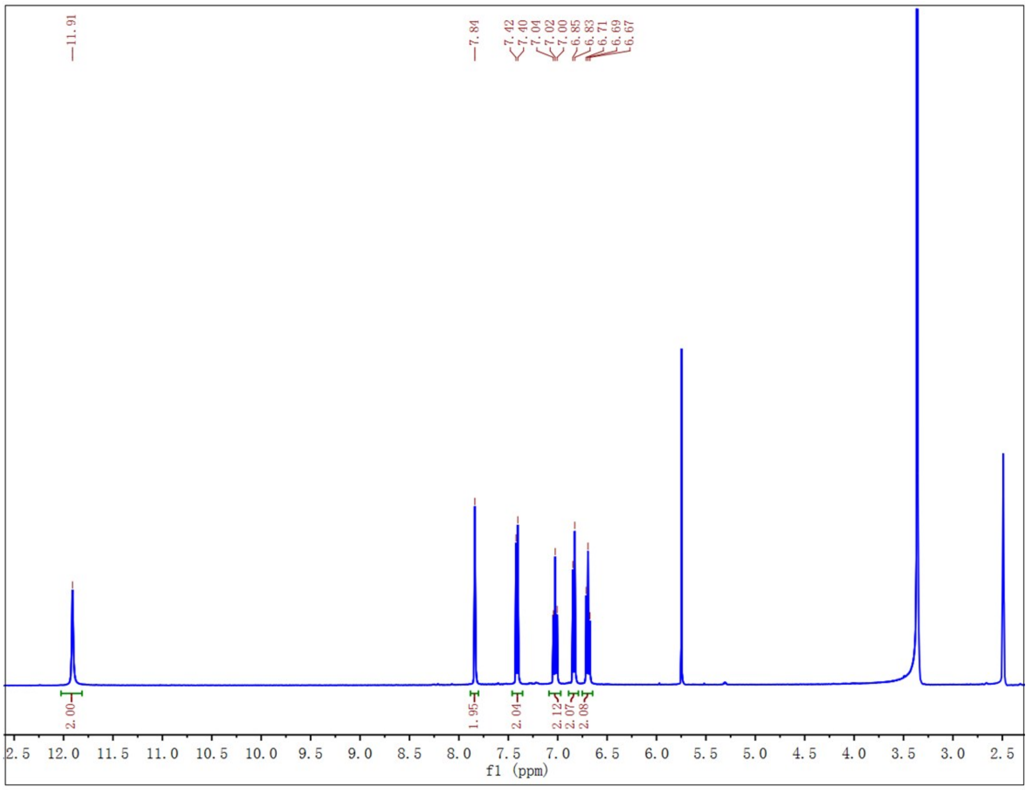

Fig. S32 ^{1}H NMR of BIMA in *d*-DMSO.

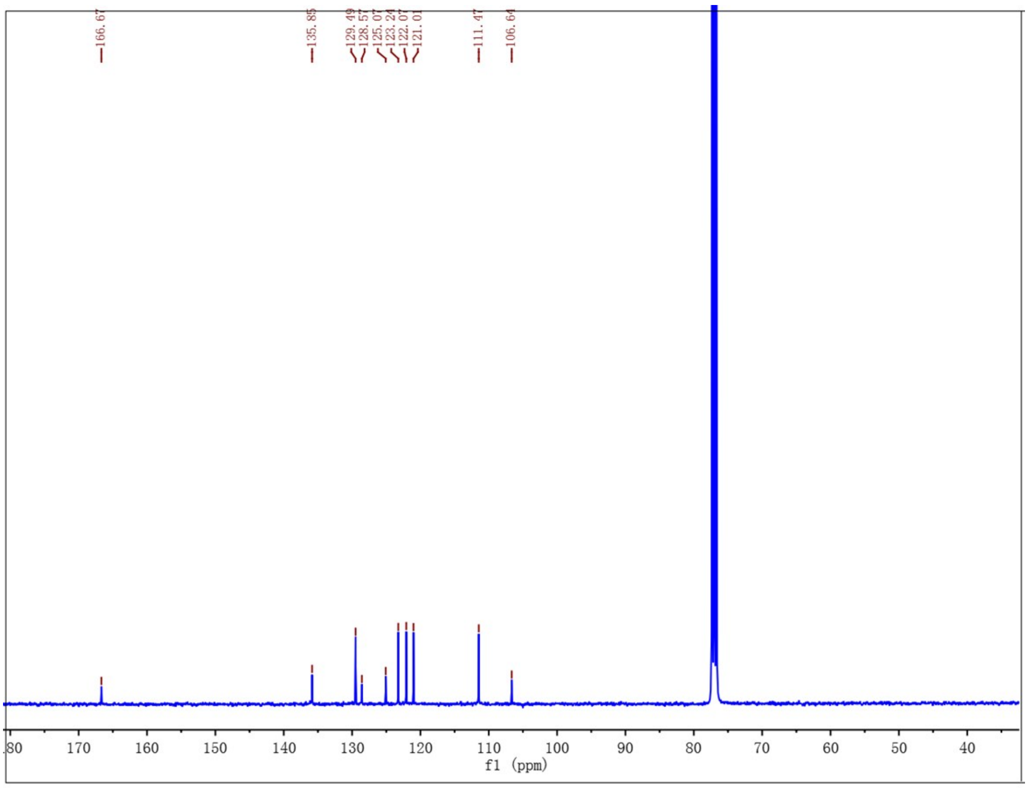

Fig. S33 ^{13}C NMR of BIMA in *d*-$CDCl_3$.

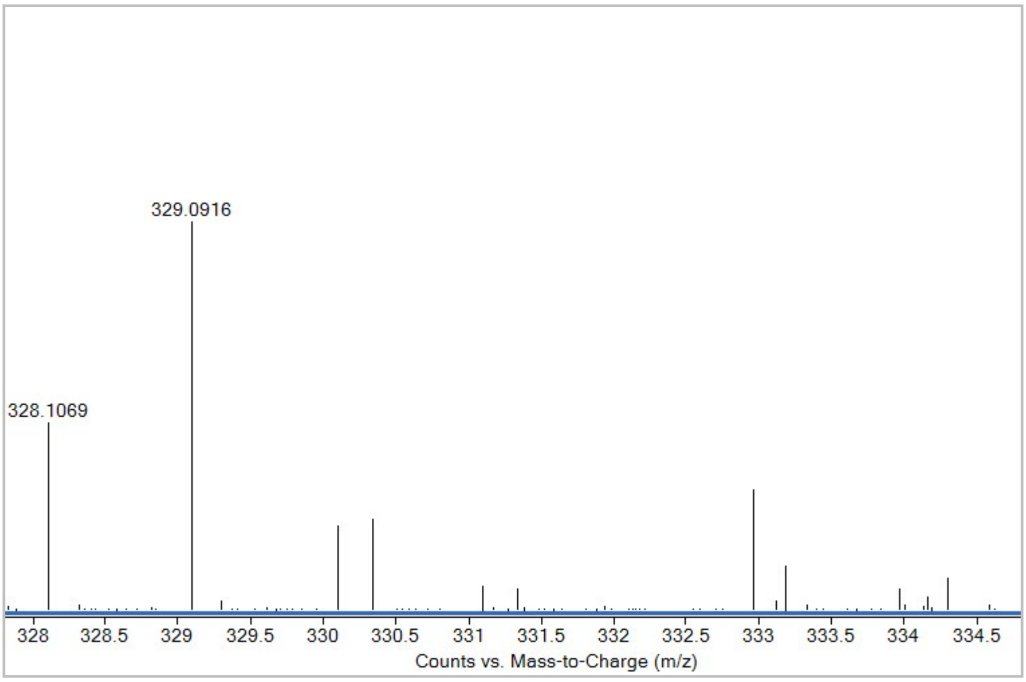

Fig. S34 High-resolution Mass of BIMA.

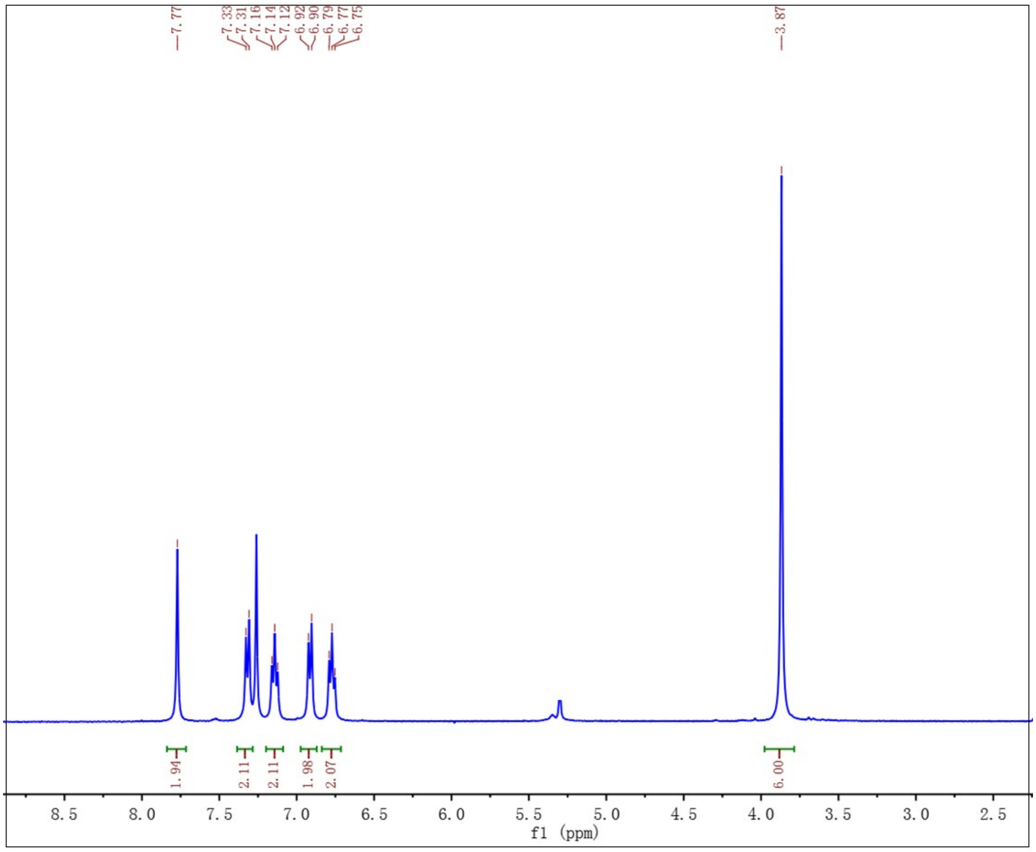

Fig. S35 ^{1}H NMR of BIMA-M in *d*-$CDCl_3$.

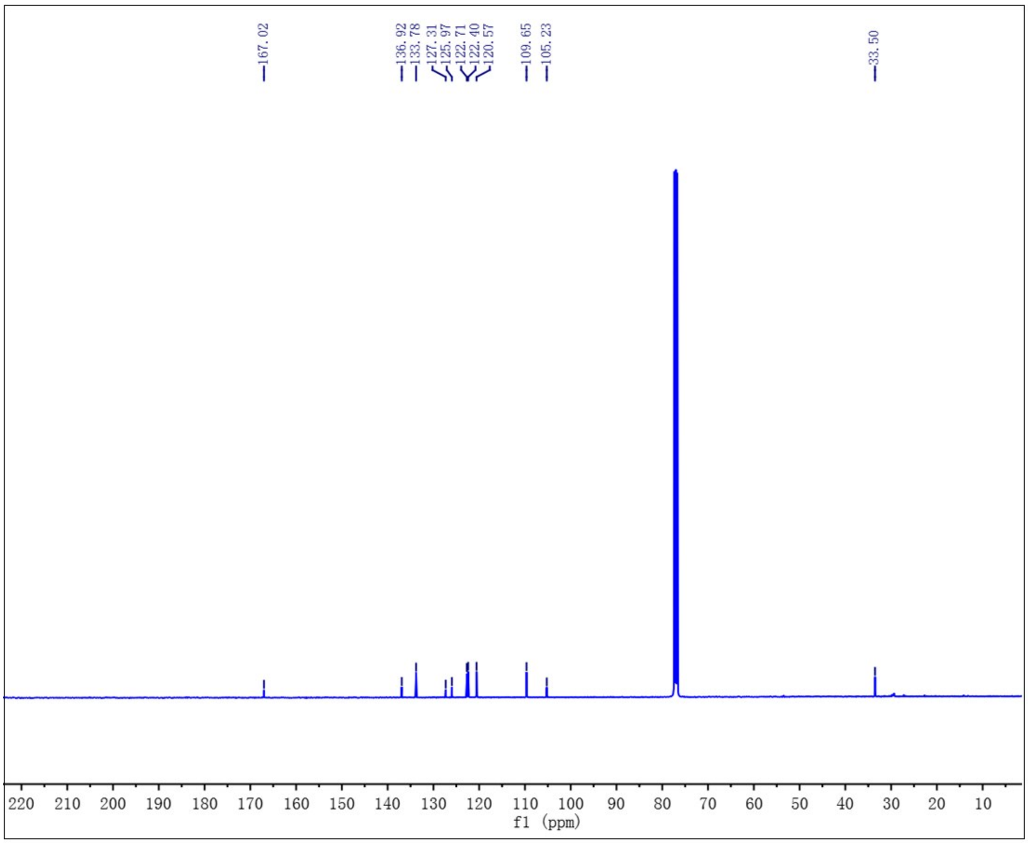

Fig. S36 ^{13}C NMR of BIMA-M in *d*-$CDCl_3$.

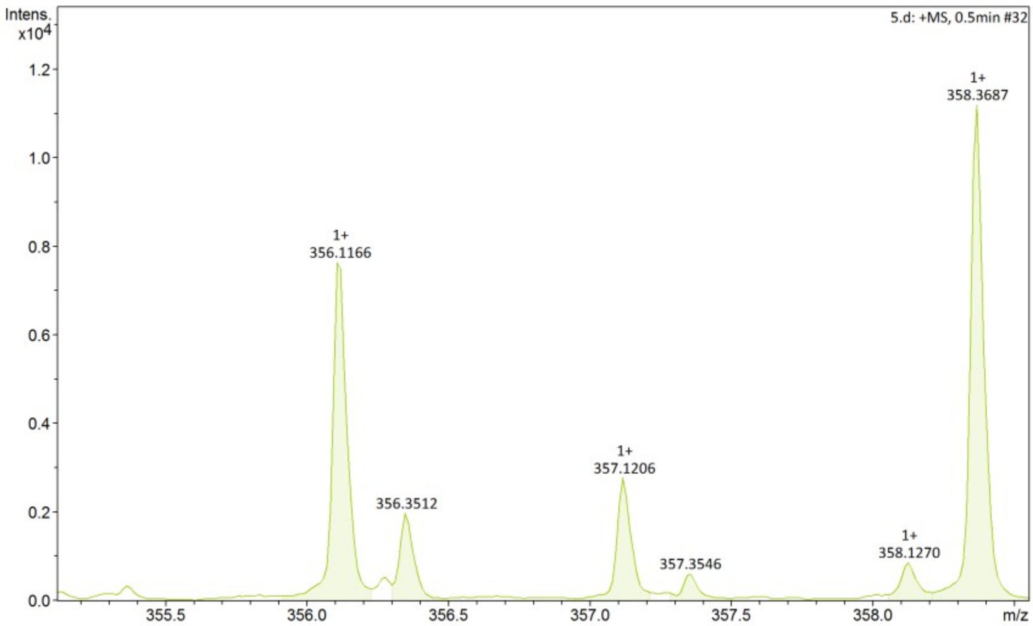

Fig. S37 High-resolution Mass of BIMA-M.

4. References

1 W. H. Melhuish, *J. Phys. Chem.* 1961, **65**, 229-235.

2 M. J. Frisch, G. W. Trucks, H. B. Schlegel, G. E. Scuseria, M. A. Robb, J. R. Cheeseman, J. A. Montgomery, Jr., T. Vreven, K. N. Kudin, J. C. Burant, J. M. Millam, S. S. Iyengar, J. Tomasi, V. Barone, B. Mennucci, M. Cossi, G. Scalmani, N. Rega, G. A. Petersson, H. Nakatsuji, M. Hada, M. Ehara, K. Toyota, R. Fukuda, J. Hasegawa, M. Ishida, T. Nakajima, Y. Honda, O. Kitao, H. Nakai, M. Klene, X. Li, J. E. Knox, H. P. Hratchian, J. B. Cross, V. Bakken, C. Adamo, J. Jaramillo, R. Gomperts, R. E. Stratmann, O. Yazyev, A. J. Austin, R. Cammi, C. Pomelli, J. Ochterski, P. Y. Ayala, K. Morokuma, G. A. Voth, P. Salvador, J. J. Dannenberg, V. G. Zakrzewski, S. Dapprich, A. D. Daniels, M. C. Strain, O. Farkas, D. K. Malick, A. D. Rabuck, K. Raghavachari, J. B. Foresman, J. V. Ortiz, Q. Cui, A. G. Baboul, S. Clifford, J. Cioslowski, B. B. Stefanov, G. Liu, A. Liashenko, P. Piskorz, I. Komaromi, R. L. Martin, D. J. Fox, T. Keith, M. A. Al-Laham, C. Y. Peng, A. Nanayakkara, M. Challacombe, P. M. W. Gill, B. G. Johnson, W. Chen, M. W. Wong, C. Gonzalez and J. A. Pople, GAUSSIAN 09 (Revision B.01), Gaussian, Inc., Wallingford, CT, 2004.

3 X. Li, J. Chen, D. Ma, Q. Zhang, H. Tian, *Proc. of SPIE*, 2005, **5632**, 357-364.